Accepted Manuscript

Ciprofloxacin by-products in seawater environment in the presence and absence of gilt head bream

Haizea Ziarrusta, Leire Mijangos, Mireia Irazola, Ailette Prieto, Nestor Etxebarria, Eneritz Anakabe, Maitane Olivares, Olatz Zuloaga

PII: S0045-6535(18)30069-9

DOI: 10.1016/j.chemosphere.2018.01.069

Reference: CHEM 20650

To appear in: *ECSN*

Received Date: 22 November 2017

Revised Date: 3 January 2018

Accepted Date: 13 January 2018

Please cite this article as: Ziarrusta, H., Mijangos, L., Irazola, M., Prieto, A., Etxebarria, N., Anakabe, E., Olivares, M., Zuloaga, O., Ciprofloxacin by-products in seawater environment in the presence and absence of gilt head bream, *Chemosphere* (2018), doi: 10.1016/j.chemosphere.2018.01.069.

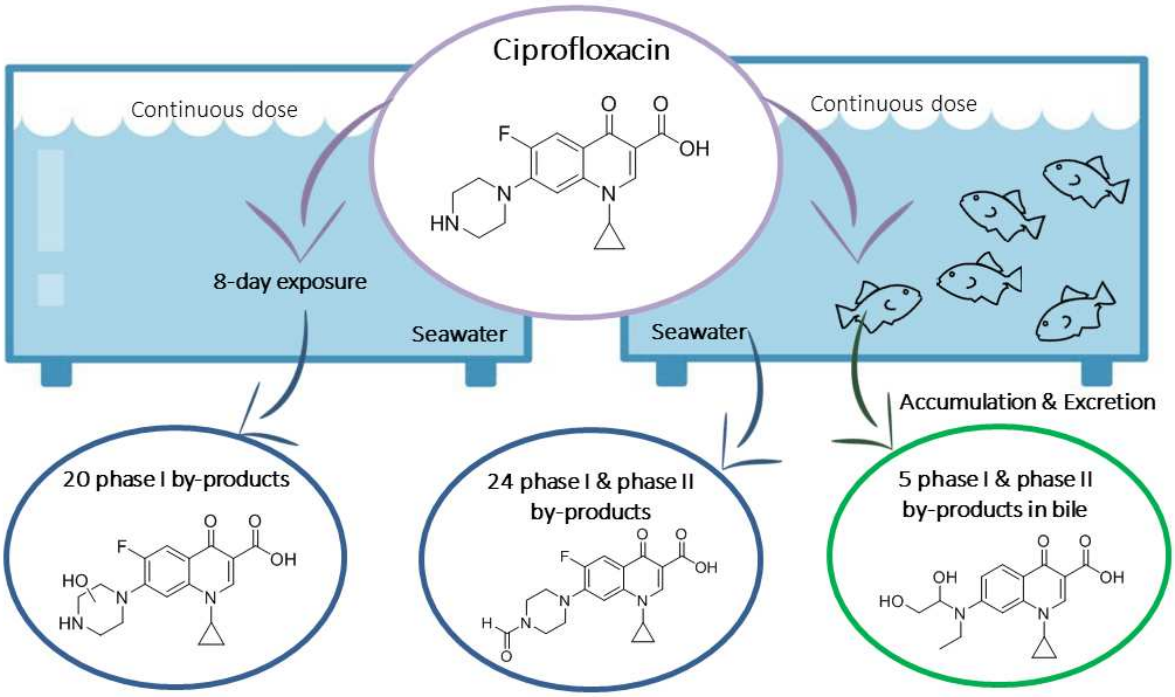

Ciprofloxacin By-Products in Seawater Environment in the Presence and Absence of Gilt Head Bream

Haizea Ziarrusta[1], Leire Mijangos[1], Mireia Irazola[1,2], Ailette Prieto[1,2], Nestor Etxebarria[1,2], Eneritz Anakabe[3], Maitane Olivares[1,2], Olatz Zuloaga[1,2]

1. Department of Analytical Chemistry, University of the Basque Country (UPV/EHU), Leioa, Basque Country, Spain

2. Research Centre for Experimental Marine Biology and Biotechnology (PIE), University of the Basque Country (UPV/EHU), Plentzia, Basque Country, Spain

3. Department of Organic Chemistry, University of the Basque Country (UPV/EHU), Leioa, Basque Country, Spain

*****Corresponding author: Haizea Ziarrusta (haizea.ziarrusta@ehu.eus)

Department of Analytical Chemistry, Faculty of Science and Technology, University of the Basque Country (UPV/EHU), P.O. Box 644, 48080 Bilbao, Spain.

Tel: + 34 94 601 55 51; Fax: +34 94 601 35 00

Abstract

The widespread use of pharmaceuticals has caused a growing concern on the presence of pharmaceuticals such as the antibiotic ciprofloxacin (CIPRO) in the aquatic environment, since they may exert adverse effects on non-target organisms, including fish. In order to study the uptake, distribution in different tissues (liver, muscle, brain and gill) and biofluids (plasma and bile), metabolism and elimination of CIPRO in gilt-head bream (*Sparus aurata*), controlled dosing experiments for 8 days at 200 µg/L concentration were carried out. CIPRO was only observed in bile at concentration up to 315 ± 4 ng/mL, probably due to its low octanol-water partition coefficient (log P = -2.4 at pH 7.4) and the zwitterionic behavior (pKa_1 = 5.76 and pKa_2 = 8.68). CIPRO by-products (BPs) were also identified in seawater environment, both in presence and absence of fish. The analysis done by means of liquid chromatography–high resolution mass spectrometry (hybrid quadrupole-Orbitrap) permitted the annotation of up to 35 BPs of CIPRO in seawater and bile, from which 30 structures were reported for first time. These results confirm that CIPRO is very susceptible to photolysis, and that it goes through various phase I and phase II metabolisms in the fish. All these results suggested that, for a complete characterization of CIPRO exposure, BPs should also be included in the biomonitoring campaigns since they might also be toxicologically relevant.

Keywords: Ciprofloxacin, seawater, gilt-head bream, by-products, high-resolution mass spectrometry

1. INTRODUCTION

There is a growing concern on the presence of pharmaceutical active compounds (PhACs) in the environment since they may exert adverse effects on non-target organisms after they enter into the ecosystems (Babić et al., 2013; Van Doorslaer et al., 2014; Zhao et al., 2015). Among PhACs, special attention has been paid to antibiotics specially due to the rapid expansion of antibiotic resistance observed since the late 90's (Aryal, 2001; Carvalho and Santos, 2016; Levy, 1997, 2002). Due to their high use and continuous release to the environment, their transformation and elimination rate is balanced and antibiotics are, therefore, known as "pseudo-persistent" pollutants (Maia et al., 2014).

Fluoroquinolones (FQs) are a class of antibiotics used against respiratory diseases and bacterial infections in human and veterinary medicine (Alcaráz et al., 2014; Ashfaq et al., 2016; Babić et al., 2013; Turiel et al., 2005). Due to the widespread application of FQs such as ciprofloxacin (CIPRO), and the fact of being partially metabolized in the body and not completely removed in wastewater treatment plants, FQs are the most detected antibiotics in the environment, at concentrations in the ng/L-µg/L range in aquatic ecosystems, which may act as sinks for antibiotics through different pathways such as domestic/municipal wastewaters, surface waters and hospital effluents (Babić et al., 2013).

FQs are resistant to hydrolysis and elevated temperatures but they can absorb UV radiation and are photodegradable (Babić et al., 2013). Although CIPRO is threatening the aquatic organisms at actual environmental concentrations (Gomes et al., 2017), little is known on its distribution, metabolism and elimination in tissues of aquatic organisms.

The determination of antibiotics and their by-products (BPs), namely metabolites and transformations products (TPs), is relevant to establish the sources, transport, fate and effects in the environment (Carvalho and Santos, 2016). High-resolution mass spectrometry (HRMS) plays an important role on the determination of BPs. The high resolution/high mass accuracy, exact mass and isotopic profile measurements performed by HRMS allow inferring the unequivocal molecular formula. When full MS data information is complemented with the MS2 spectra obtained in hybrid mass spectrometers, tentative structure candidates can be proposed for the BPs (Schymanski et al., 2014).

In this framework, the aim of the present work was to study the uptake, distribution and metabolization of CIPRO in tissues (brain, liver, gill, muscle) and biofluids (plasma, bile) of juvenile gilt-head bream (*Sparus aurata*). Controlled dosing experiments were performed in the presence and absence of fish in seawater, and the HRMS analysis of the different matrices was performed in a hybrid quadrupole-Orbitrap mass spectrometer to annotate the BPs generated under each condition.

2. MATERIALS AND METHODS

2.1. Standards and Reagents

CIPRO (98%) and [$^{2}H_{8}$]-ciprofloxacin ([$^{2}H_{8}$]-CIPRO, 99.6%) were purchased from Sigma-Aldrich (St. Louis, MO, USA). CIPRO stock solution was prepared at 500 mg/L in methanol (MeOH, Fisher Scientific, Loughborough, UK) and CIPRO dosing solution was prepared in Milli-Q water at 45.2 mg/L. In both cases sodium hydroxide (NaOH, ≥ 99%, Merck, Darmstadt, Germany) was added to ease

CIPRO dissolution. Stock solutions were stored in the darkness at −20 ℃. For the other standards and reagents information see Supplementary Information (SI).

2.2. Metabolite and BP identification experiments

For exposure experiments, juvenile gilt-head bream, weighing around 40 g and measuring ~ 13 cm in length, were used. Fish were obtained from Groupe Aqualande (Roquefort, France) and shipped to the Marine Research Centre of Plentzia (UPV/EHU) to perform the experiments at controlled temperature (18 ℃) and light (14:10 h light:dark cycles). Fish were acclimatized for 3 months upon arrival and stabilized for an additional 1 week in the dosing tank before starting the exposure. The water was continuously aerated using aquarium oxygenators and fish were fed daily with 0.10 g pellets/fish. Water temperature (13 ℃) and pH (7.4 ± 0.3) were constant during the exposure. Dissolved oxygen, nitrite, nitrate and ammonium content were periodically monitored.

An 8-day exposure experiment was designed to identify BPs of CIPRO. Four 1000 × 700 × 650 mm polypropylene tanks containing 250 L of seawater were used: two of them contained 40 fish each and the other two only seawater. One of the tanks containing fish and one of the tanks without fish were continuously fortified at 200 ng/mL (nominal concentration), whereas the other tanks were used as control (one with fish, one without fish).

CIPRO dosing was performed using a continuous flow-through system with a peristaltic pump delivering 9 L seawater/h and another pump infusing CIPRO dosing solution (45.2 mg/L, refilled every 24 h with newly prepared solution) at 40 mL/h to exposure tank. Control tanks were maintained at identical conditions over the duration of the experiment but only seawater was delivered.

2.3. Sample Collection

Fish handling and dissection were performed according to the Bioethics Committee rules of UPV/EHU (procedure approval CEEA/380/2014/ETXEBARRIA LOIZATE). 10 fish were collected from control and exposed tanks on exposure days 0 (before exposure), 1, 3 and 8. The fish were immediately anaesthetized in a tank holding 10 L of seawater containing tricaine and $NaHCO_3$, both at 200 mg/L. After 5 min, fish were length measured, weighed and dissected to collect tissues (brain, gill, liver, muscle) and biofluids (bile, plasma). Blood was taken from the caudal vein-artery using a syringe (previously homogenized with 0.5 mol/L EDTA solution at pH 8.0) and then, centrifuged for 7 min at 1000 rpm to get the plasma. Biofluids and fish tissues were snap-frozen and kept in liquid nitrogen during dissection and stored at -80 ℃ freezer prior to an alysis.

At the time that fish were removed from the tanks, 2-L water samples were also collected from the four tanks to determine the concentration of CIPRO and to identify CIPRO BPs in water. Water samples were extracted and analyzed within 24 h.

2.4. Sample Handling

Fish tissues (brain, gill, liver, muscle) were freeze-dried for 48 h using a Cryodos-50 laboratory freeze-dryer (Telstar Instruments, Sant Cugat del Valles, Barcelona, Spain). A homogenized pool was prepared for each tissue/biofluid using the 10 fish collected at each sampling day. The pools and the seawater samples (100 mL) were extracted and analyzed in triplicate using a previously developed analytical method (Ziarrusta et al., 2017). Procedural blanks were analyzed to

discard chromatographic peaks associated to contaminations during the identification of BPs.

2.5. Instrumental Analysis

CIPRO was quantified by liquid chromatography tandem mass spectrometry (LC-QqQ-MS/MS) using a previously developed method (Ziarrusta et al., 2017). BP identification was performed using a Thermo Scientific Dionex UltiMate 3000 UHPLC coupled to a Thermo Scientific Q Exactive quadrupole-Orbitrap mass spectrometer equipped with a heated ESI source (HESI, Thermo, CA, USA). For HRMS measurement information see SI.

2.6. Data Handling

CIPRO was quantified using a 10-point external calibration curve whereas BPs were identified using Compound Discoverer 2.0 (Thermo). For peak picking, peak alignment and peak annotation criteria see SI.

3. RESULTS AND DISCUSSION

3.1. CIPRO accumulation in fish

Condition factor (K = (fish weight x 100)/length^3) and hepatic somatic index (HSI = (liver weight x 100)/fish weight) were calculated to assess general fish health (Nallani et al., 2016). Mortality was not observed in any of the experiments and K and HSI values were not statistically different between control and exposed ($p = 0.95$ and $p = 0.78$, respectively), indicating maintenance of fish health during the exposure.

The average concentration of CIPRO in seawater was consistent with the nominal dosing concentration (200 ng/mL) regardless the absence (235 ± 20 ng/mL) or

158 presence (208 ± 3 ng/mL) of fish. The concentration of CIPRO in samples
159 collected before starting the exposure (day 0) and in samples from all control tanks
160 was bellow method detection limit (MDL, 2 ng/L, (Ziarrusta et al., 2017)).

161 Regarding the uptake in fish, CIPRO was only detected in bile whereas it was
162 under MDLs in the rest of analyzed fish biofluid and tissues regardless the
163 exposure time.

164 The concentrations of CIPRO in bile increased over the exposure time:
165 74 ± 14 ng/mL, 124 ± 30 ng/mL and 315 ± 4 ng/mL (at 95% of confidence level) in
166 sampling days 1, 3 and 8, respectively. Low uptake factors for CIPRO were also
167 found in the literature in comparison to other non-ionizable pollutants (Gao et al.,
168 2012). The low octanol-water partition coefficient (log P:-2.4 at pH:7.4) and the
169 zwitterionic behavior of CIPRO may reduce its uptake rate and accumulation
170 capacity in lipidic tissues. However, its bioavailability and accumulation in biofluids
171 (such as bile) can be increased due to the larger transfer capacity across cell
172 membrane of the ionized form of the compound (Erickson et al., 2006). Moreover,
173 saline environment can also reduce the accumulation factors of the drug, since
174 some FQs are apparently worse absorbed by fish in saline environment (Elston et
175 al., 1994). Finally, the metabolization of CIPRO should be also suggested to
176 explain its low accumulation since it is susceptible to photolysis by dealkylation,
177 defluorination and hydroxylation (Turiel et al., 2005). CIPRO can go through
178 various phase I and II metabolisms after entering into fish body and its
179 accumulation without any transformation can be also reduced (see discussion in
180 section 3.2).

181 **3.2 CIPRO BPs**

BPs of CIPRO were studied in seawater (in the presence and absence of fish) and in biological tissues (liver, brain, muscle, gill) and fluids (plasma, bile). Table S2 includes the molecular formula, the theoretical *m/z* of the $[M+H]^+$ form and the corresponding ΔMass (ppm) for each matrix, the most abundant fragments in the MS2 spectra and the retention time for CIPRO and all identified BPs (see MS2 spectra in Fig. S1).

CIPRO fragmentation is conditioned by the two charge isomers, namely CIPRO A and CIPRO B (see Fig. S2), which show different collision induced dissociation (CID) spectra (Kovačević et al., 2014). CIPRO A corresponds to the isomer where the charge resides in the piperazinyl ring and CIPRO B to the isomer when the proton resides in keto group. CIPRO A fragmentation begins with a CO_2 neutral loss and CIPRO B loses first H_2O (Kovačević et al., 2014)

a) BPs in water in the absence of fish

In a first approach BPs in the absence of fish were studied due to the susceptibility towards photolysis shown by CIPRO (Burhenne et al., 1997; Pereira et al., 2007; Vasconcelos et al., 2009). Up to 20 BPs (see Fig. 1) were observed and 16 were reported for the first time.

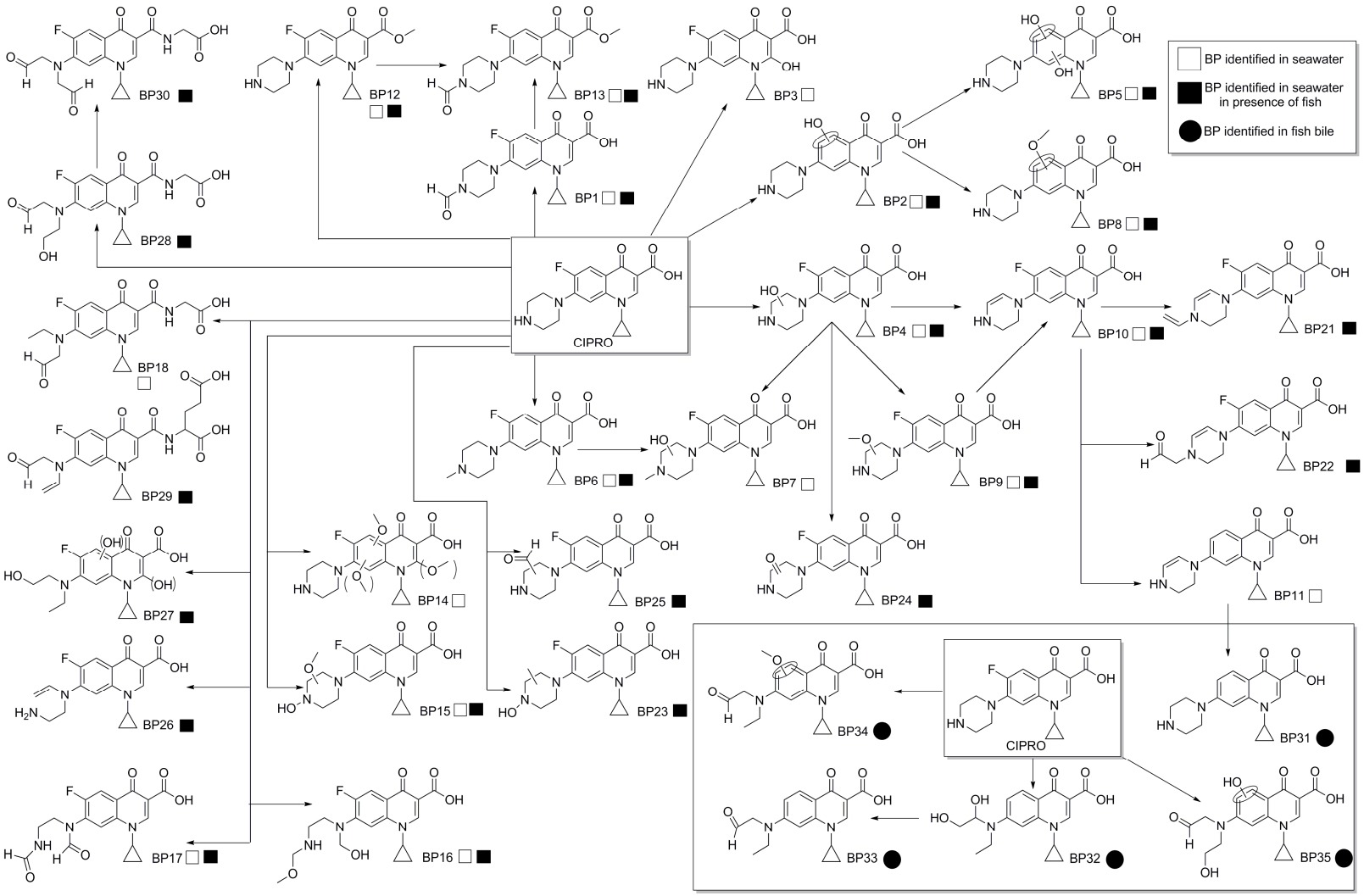

Fig. 1. Proposed degradation pathway of CIPRO in seawater (in the absence and presence of gilt-head bream fish) and in fish bile.

BP1 (*m/z* 360.13541) showed a composition change of +CO with respect to CIPRO. The absence of *m/z* 70 (C_4H_8N) indicated that the modification occurred in the piperazinyl ring. The *N*-formylation of CIPRO could explain the basicity loss of the secondary nitrogen and the favored equilibrium towards the equivalent of CIPRO B structure, as pinpointed by the water loss observed in fragment *m/z* 342. Additionally, the abundant ion *m/z* 243 ($C_{13}H_8FN_2O_2$) suggested the loss of C_5H_9NO moiety (*m/z* 99) in the piperazinyl ring from the dehydratated fragment (*m/z* 342). This BP was previously described in the literature (Haddad and Kümmerer, 2014; Morales-Gutiérrez et al., 2014).

BP2-BP4 consisted on monohydroxylated derivatives of CIPRO. BP2 (*m/z* 330.14484), an oxidative defluorination of CIPRO, has been widely described in the literature (Guo et al., 2013; Haddad and Kümmerer, 2014; Paul et al., 2010; Vasconcelos et al., 2009; Villegas-Guzman et al., 2017; Wetzstein et al., 1999). The much lower abundance of fragment *m/z* 286 (loss of CO_2) than fragment *m/z* 312 (loss of water) pinpointed that the equivalent structure of CIPRO B was favored. Fragments *m/z* 70, 217, 231, 243 and 312 indicated that an oxidation had caused the loss of the fluorine atom through a nucleophilic aromatic substitution. The lack of loss of water, together with defluorination, pinpointed that the hydroxyl group was introduced in the aromatic ring. However, with the data available, it was not possible to assign the position of the hydroxyl group in the aromatic ring, which could be located in the position left by the fluorine atom or in the adjacent carbon (Ramanathan et al., 2005). BP3 (*m/z* 348.13541) also corresponded to the hydroxylation of CIPRO but without defluorination. The presence of *m/z* 70 showed that the piperazinyl ring was unmodified. Similar to BP2, the lack of loss of water suggested that the hydroxyl group was located at any carbon with sp^2

hybridation. However, fragment *m/z* 305 ($C_{15}H_{14}FN_2O_4$), with all oxygen atoms and one nitrogen atom less than the precursor (m/z 305=348-C_2H_5N), pinpointed that the piperazinyl ring was broken before common dehydration or decarboxylation in the carboxylic group. This difference could be caused if the hydroxyl group was placed in the carbon with the sp^2 hybridation in the piperidin-4-one ring as reported in the literature (Guo et al., 2013; Haddad and Kümmerer, 2014). Finally, for BP4 (*m/z* 348.13541), the absence of fragment *m/z* 70 and the presence of two losses of water (fragment *m/z* 272 corresponded to the loss of two water molecules of the precursor together with the loss of the cyclopropyl group) suggested that the hydroxylation occurred in the piperazinyl ring. Moreover, the presence of fragments *m/z* 272 ($C_{14}H_{11}FN_3O_2$) and *m/z* 285 ($C_{16}H_{16}FN_3O$), both maintaining all the N atoms of CIPRO, indicated that this hydroxylation could increase the stability of the piperazinyl ring since the characteristic fragments of piperazinyl ring cleavage in CIPRO (*m/z* 231, 249 and 217) were not detected.

A single dihydroxylated BP of CIPRO was observed, BP5 (*m/z* 346.13975), which could correspond to an oxidative defluorination plus a second hydroxylation of CIPRO. The presence of *m/z* 70 indicated that the piperazinyl ring was unmodified. Similarly to BP2, fragments *m/z* 328 (loss of water) and *m/z* 300 (loss of CO) pinpointed that the equivalent structure of CIPRO B was favored, and both –OH groups should be placed in the aromatic ring for larger structural stability. One of the hydroxyl groups should be placed in replacement of the fluorine atom or in the adjacent sp^2 carbon atom, but the position of the second hydroxyl group could not be determined. We discarded that the second hydroxyl group was located at the sp^2 carbon atom in the piperidin-4-one ring since fragment *m/z* 303, corresponding to $C_{15}H_{16}N_2O_5$ and equivalent to fragment *m/z* 305 observed in BP3, was not

observed. Similar BPs with two hydroxyl groups in the aromatic ring have been previously described in the literature (Haddad and Kümmerer, 2014; Wetzstein et al., 1999).

N-methylation of CIPRO was observed in BP6. The absence of *m/z* 70 suggested that the methylation of CIPRO occurred in the piperazinyl ring. Furthermore, the precursor ion *m/z* 346.15615 was almost completely fragmented and the rest of fragments (*m/z* 332, 314, 312, 249, 231) corresponded to common CIPRO fragmentation. In the case of BP7 (*m/z* 362.15106), hydroxylation plus methylation of CIPRO occurred. The absence of fragment *m/z* 70, and the presence of *m/z* 86 (C_4H_8NO) indicated a modification of the piperazinyl ring by the addition of a hydroxyl group and a methyl group. Similar to BP6, demethylation (*m/z* 348) was observed in the fragmentation, and the ion *m/z* 330 ($C_{17}H_{17}FN_3O_3$) could correspond to the dehydration of the demethylated fragment rather than to the loss of a methoxy group (-32) from the parent *m/z* 362. In addition, similar to BP4, the presence of fragment *m/z* 272, indicating that something had stabilized the piperazinyl ring, pinpointed that BP7 could be either the methylation product of BP4 or the hydroxylation product of BP6.

Methoxylation of CIPRO was observed in both BP8 and BP9. BP8 (*m/z* 344.16049) showed both the gain of a methoxy group and the loss of the fluorine atom. Therefore, the most plausible structures were the oxidative replacement of the fluorine atom with the methoxy group or the methoxylation of the adjacent sp^2 carbon atom (Ramanathan et al., 2005). This is in agreement with the presence of *m/z* 70 fragment and the lack of a methoxy group loss. Moreover, the loss of water (*m/z* 326) and the decarboxylation (*m/z* 300) suggested that neither the carboxylic group nor the secondary amine of the piperazinyl ring were modified and that the

protonation was in equilibrium between these two functional groups. In the case of BP9 (*m/z* 362.15106), in contrast with BP7 and BP8, a loss of a methoxy group was detected in the fragmentation pattern (*m/z* 330). The absence of fragment *m/z* 70 and the presence of *m/z* 68 pinpointed that an unsaturation ($-H_2$) appeared in the piperazinyl ring during fragmentation, most probably during the loss of the methoxy group. Furthermore, fragment *m/z* 86 (C_4H_8NO) could be explained by the presence of the methoxy group in the piperazinyl ring. Lastly, the abundant fragment *m/z* 302 belongs to C_2H_4 loss after demethoxylation.

In the case of BP10, the precursor ion *m/z* 330.12485 contained one unsaturation ($-H_2$) more than CIPRO. The absence of fragment *m/z* 70 and the presence of *m/z* 68 pinpointed that the unsaturation should be located in the piperazinyl ring, caused after dehydration of BP4 or demethoxylation of BP9. The higher stability of alkene function compared to imine group pinpoints that the unsaturation should be located between two carbon atoms. A regioisomer of BP10 with the unsaturation in the imine group has been previously described in the literature (Salma et al., 2016). Similar to BP10, BP11 (*m/z* 312.13427) also contained an unsaturation more than CIPRO but in this case defluorination had also taken place. The absence of the fragment *m/z* 70 and the presence of *m/z* 68 pinpointed that the unsaturation should be placed in the piperazinyl ring.

Esterification of CIPRO was also observed in BPs 12 and 13 of CIPRO. In the case of BP12, the precursor ion *m/z* 346.15615 pinpointed the addition of CH_2 in the molecule. Similar to BP6, the MS2 spectra contained abundant fragments (*m/z* 332, 314, 312, 249, 245, 231) also present in CIPRO. However, compared to BP6, the presence of the fragment *m/z* 70 suggested that the piperazinyl ring was unmodified and esterification in the carboxylic group of CIPRO was the most

tentative structure. However, BP13 (*m/z* 374.15106) could correspond to the *N*-formylation of BP12 or esterification of BP1 since, once the methyl group was lost (*m/z* 360), the fragmentation pattern (*m/z* 342, 231, 243) corresponded to BP1.

Dimethoxylation of CIPRO was observed in BP14. The presence of the fragments *m/z* 70 and *m/z* 348, indicating the decarboxylation of the precursor ion *m/z* 392.16163, pinpointed that the piperazinyl ring was unmodified. The composition change $+C_2H_4O_2$ could come from the introduction of two methoxy groups in CIPRO. However, since only a small fragment showing the methoxy loss was observed (*m/z* 360), the methoxy groups should be located in carbons with sp^2 hybridation, at least one in the aromatic ring and the second one also in the aromatic ring or in the piperidin-4-one ring. Abundant fragment *m/z* 227.11816 could not be explained due to the absence of a molecular formula related with CIPRO that could explain that exact mass.

Although the MS2 spectrum of BP15 was quite poor, the fragment *m/z* 346 corresponded to the loss of a methoxy group from the precursor *m/z* 378.14598. Compared to CIPRO, BP15 contained one more oxygen atom and an unsaturation, which could be explained if the methoxy group was located on the piperazinyl ring and generated an unsaturation when fragmented. This is in agreement with the absence of the *m/z* 70 fragment. Furthermore, after demethoxylation, a small fragment, corresponding to a water loss (*m/z* 328), and a lack of decarboxylation were observed, suggesting that *N*-hydroxylation occurred in the secondary amine group to favor the positive charge equilibrium to the oxygen atom in the piperidin-4-one ring.

BP16-BP18 had undergone the cleavage of the piperazinyl ring, which has been previously described in the literature (Haddad and Kümmerer, 2014; Villegas-

Guzman et al., 2017; Guo et al., 2013; Hu et al., 2011; Morales-Gutiérrez et al. , 2014; Paul et al., 2010; Salma et al. 2016; Vasconcelos et al., 2009; Zhang et al., 2015; Prieto et al., 2011; Babić, et al.,2013; Maia et al,. 2014). BP16 (*m/z* 380.16163) could correspond to the methoxylation and hydroxylation of CIPRO after the cleavage of the piperazinyl ring. The loss of a methoxy group was clearly observed (*m/z* 348), which could be located in the *N*-methyl moiety formed after the cleavage of the piperazinyl ring due to the presence of fragment *m/z* 86 (C_4H_8NO) instead of the fragment *m/z* 70, similar to BP9. On the other *N*-methyl group, obtained after the cleavage of the piperazinyl ring, hydroxylation is proposed in order to explain the presence of the fragment *m/z* 72 (CH_3H_6NO). After demethoxylation, water loss (*m/z* 330) and defluorination (*m/z* 328) were observed in the spectrum. Villegas et al. (Villegas-Guzman et al., 2017) described a similar BP, but with two hydroxyl groups in the structure. In the case of BP17, the precursor ion *m/z* 362.11468 contained two more oxygen atoms and a single unsaturation. The lack of *m/z* 70 suggested that the piperazinyl ring had been modified. Furthermore, the CO loss before the water loss (*m/z* 334) suggested the presence of at least an aldehyde group. In the absence of a dehydration and in the presence of fragment *m/z* 72 (C_3H_6NO), one possible structure could contain two aldehyde groups after the cleavage of the piperazinyl ring, as already described in the literature (Hu et al. 2011; Paul et al., 2010), and the MS2 fragments observed, including *m/z* 334, 316, 299, 273, 259 and 245, matched with the reported values. Finally, according to the Compound Discoverer 2.0 program, BP18 (*m/z* 390.14598) corresponded to the oxidative deamination to alcohol plus glycine conjugation of CIPRO. Glycine conjugation in the carboxylic acid group of acidic xenobiotics and oxidative deamination of primary amines are common phase II

and phase I reactions, respectively (Hop and Prakash, 2005). In the case of CIPRO, a previous cleavage of the piperazinyl ring is required to form the primary amine. This structure is also in agreement with the lack of fragment *m/z* 70.

BP19 (*m/z* 344.10411, $C_{17}H_{14}FN_3O_4$) contained 4 hydrogen atoms less and an oxygen atom more than CIPRO. The presence of fragment *m/z* 70 suggested no modification in the piperazinyl ring. On the other hand, the loss of water (*m/z* 326) and the consecutive CO loss (*m/z* 298) were attributed to the carboxylic group. Therefore, the most probable position to add an unsaturation and the keto group was the cyclopropyl ring, which was supported by the presence of the fragment *m/z* 53 (C_3HO). However, it was not possible to determine if this oxidation involved the cleavage of the cyclopropyl moiety since it is not common in literature.

Finally, the structure of BP20 (*m/z* 360.17180) showed a $+C_2H_4$ composition change compared to CIPRO, but the structure could not be annotated since we did not observe neither a methyl or ethyl loss in the fragmentation, nor a modification of the piperazinyl ring (*m/z* 70), but a decarboxylation (*m/z* 316) of the precursor ion.

Oxidation, methylation (*N*-, *C*- or *O*-methylation), oxidative defluorination (in 3 BPs out of 20), reductive defluorination (1 BP our of 20), dehydrogenation of the piperazinyl ring (in 2 BPs) and the cleavage of the piperazinyl ring with (1 BP) or without (2 BPs) the loss of the primary amine formed during the cleavage were the main phase I transformations of CIPRO in seawater. The only phase II transformation of CIPRO observed was BP18, which suffered oxidative deamination of the piperazinyl ring and glycine conjugation. Regarding toxicology of the BPs, even though most of the annotated BPs were identified in the present work were for the first time and scarce information is found in the literature,

Toolaram and co-workers reported that BP2, BP5 and BP17 may be genotoxic to bacteria and mammals according to QSAR (Quantitative Structure Activity Relationships) predictions (Toolaram et al., 2016). However, they reported that antagonistic mixture interactions or the low concentration of the BPs in the mixture was not sufficient to cause any observable effect in the bioassays (Toolaram et al., 2016).

b) BPs in water in the presence of fish

14 of the previously detected BPs were also observed (BP 1-2, 4-6, 8-10, 12-13, 15-17, 20) and 10 new BPs were annotated in seawater in presence of fish, from which 9 were reported for the first time in the present work (see Fig. 1).

In BP21, while decarboxylation of precursor ion *m/z* 356.14050 was not observed, the fragment corresponding to the dehydration (*m/z* 338) was one of the main fragments. Dehydration is common when the secondary amine of piperazinyl ring is modified. The absence of the fragment *m/z* 70 and the presence of *m/z* 68 pinpointed that the unsaturation should be in the piperazinyl ring (similar to BP10 and BP11) and fragment *m/z* 94 suggested the presence of an *N*-ethylene group. Therefore, BP21 could be the alkylation product of BP10.

Similarly, in BP22 (*m/z* 372.13541) the introduction of an unsaturation in the CIPRO structure is also required in order to explain the modification of $+C_2O$. The absence of the fragment *m/z* 70 and the presence of *m/z* 68 pinpointed that the unsaturation was located in the piperazinyl ring, similar to BPs 10, 11 and 21. Fragment *m/z* 344, due to a CO loss before dehydration (common in aldehydes), together with the presence of the abundant fragment *m/z* 110 and the presence of a water loss (*m/z* 354), related to the equivalent of CIPRO B structure, suggested

an introduction of an *N*-alkyl aldehyde group in the secondary amine of the piperazinyl ring. Therefore, BP22 could be the alkylation product of BP10.

In BP23, the precursor ion *m/z* 362.15106 was poorly fragmented and the composition change $+CH_2O$ compared to CIPRO could not be attributed to the introduction of a methoxy group because no methoxy loss was observed. The absence of fragment *m/z* 70 pinpointed that piperazinyl ring was modified and, therefore, the methoxy group could not be located in the aromatic ring. The most abundant fragment *m/z* 100 ($C_5H_{10}NO$) suggested that both transformations (methylation plus hydroxylation) should be present in the piperazinyl ring. Thus, the addition of $+CH_2O$ should be attributed to a methylation plus hydroxylation of CIPRO. The single water loss observed (m/z 344) could be attributed to the common water loss when the secondary amine group has been modified. Hence, *N*-hydroxylation of the secondary amine and methylation of a carbon atom in the piperazinyl ring was suggested to explain BP23.

BP24 (*m/z* 346.11976), a keto transformation of CIPRO, could be considered an oxidated product of the monohydroxylated BP4. The absence of *m/z* 70 indicated that the piperazinyl moiety was modified with a carbonyl group in the piperazinyl ring, as. described in the literature (Guo et al., 2013; Morales-Gutiérrez et al., 2014; Salma et al., 2016; Hu et al., 2011), and the MS2 fragments observed, including *m/z* 328, 318, 275, 257 and 229, matched with the reported values.

In BP25 (*m/z* 360.13541) fragments *m/z* 340 (360-HF) and *m/z* 332, corresponding to a CO loss before dehydration (common in aldehydes), were observed. The lack of the *m/z* 70 and the presence of fragment *m/z* 98 indicated that the aldehyde should be in the piperazinyl ring. The fragment *m/z* 68 could correspond to the aldehyde loss and the formation of an unsaturation in the

piperazinyl ring. In this case, and on contrary to BP1, the *N*-formylation of CIPRO was discarded because otherwise the equilibrium would be favored towards the equivalent of CIPRO B structure, causing a water loss not observed in BP25. Therefore, the aldehyde group should be bonded to a sp^3 carbon of the piperazinyl ring.

BP26 (*m/z* 332.14050) is a constitutional isomer of CIPRO. Although it presented similar fragmentation to CIPRO (*m/z* 314, 312, 249, 245, 231, 203), the main difference in the MS2 spectra is the absence of fragments *m/z* 70 (C_4H_8N) and *m/z* 136 (C_8H_7FN). One option to justify the lack of fragment *m/z* 70 could be the cleavage of the piperazinyl ring, giving place to an unsaturation.

BPs 27-30 suffered the oxidative deamination of the piperazinyl ring of CIPRO when fish were present. In BP27 (*m/z* 351.13508) oxidative deamination of primary amine could explain the loss of nitrogen without losing any carbon atom and, therefore, the cleavage of the piperazinyl ring was suggested followed by the oxidative deamination to alcohol. Moreover, the two methyl losses observed (fragments *m/z* 337 and *m/z* 305) could correspond to the fragmentation of the *N*-ethyl group. The second hydroxyl group added to the CIPRO structure should be in a sp^2 carbon atom since only two water losses were observed (fragments *m/z* 319 and *m/z* 287), one from the alcohol formed after oxidative deamination and the other one coming from the carboxylic group. However, there was no sufficient information in the MS2 spectra in order to locate this hydroxyl either in a sp^2 carbon atom of the aromatic ring or in the sp^2 carbon of the piperidin-4-one ring. BP28 (*m/z* 406.14089) corresponded to the combination of hydration, oxidative deamination to ketone and glycine conjugation of CIPRO. After the cleavage of the piperazinyl ring, while the primary amine suffered oxidative deamination to ketone,

the hydroxylation of the other side of the opened ring was suggested. In the MS2 fragmentation two fragments related to water loss were observed (*m/z* 388and *m/z* 370), one corresponding to the hydroxyl group in the piperazinyl side and the other one corresponding to the carboxyl group. This structure could also explain the absence of fragment *m/z* 70. Additionally, CO loss due to the presence of carbonyl group was observed in small fragments such as *m/z* 98. For BP29 (*m/z* 460.15146) an oxidative deamination plus glutamine conjugation was proposed. A large neutral CO_2 loss was observed (*m/z* 416) related to the two carboxylic groups present in glutamine. Fragment *m/z* 243 ($C_9H_{11}N_2O_6$) was also related to the glutamine conjugative. Although usually the presence of fragment *m/z* 70 is related to a lack of modification in the piperazinyl ring, this was not the case in BP29, which had suffered oxidative deamination. Finally, three transformations from CIPRO were suggested to annotate BP30 (*m/z* 404.12524) as the dehydrogenated derivate of BP28: oxidation, oxidative deamination to ketone plus glycine conjugation. However, we could not justify fragment *m/z* 306 ($C_{15}H_{17}FN_3O_3$) corresponding to the loss of $C_4H_2O_3$ from the precursor ion.

Compared to the BPs annotated in the absence of fish, oxidative deamination and both glycine and glutamine conjugation gained importance CIPRO in the presence of gilt-head bream since 4 of the 10 new BPs had suffered both transformation reactions (see Fig. 1).

c) BPs in fish tissue and fluid

Although CIPRO metabolites were searched in gilt-head bream liver, brain, muscle, gill, plasma and bile, BPs were only detected in bile and will be further commented. 5 BPs were found in fish bile and none of them was detected in seawater (see Fig. 1). The 5 new BPs, named BP31-BP35, had gone through defluorination,

475 which had only been observed in 4 of the 30 BPs previously annotated in water.
476 Moreover, all of them, except BP31, suffered oxidative deamination. Neither
477 glycine nor glutamine conjugates were observed.

478 In BP31-33 reductive defluorination took place and, in those BPs, the fluorine atom
479 was not replaced by a hydroxyl group in the aromatic ring. BP31 (*m/z* 314.14992)
480 corresponded to the reductive defluorination of CIPRO. Although the MS2 spectra
481 was poor, fragments *m/z* 296 and *m/z* 268 corresponded to the common water
482 and the consecutive CO losses. In BP32 (*m/z* 333.14450), reductive defluorination,
483 oxidative deamination and hydration of CIPRO were observed. The structure
484 shown in Fig. 1 explained the absence of the fragment *m/z* 70. The presence of
485 the abundant fragment *m/z* 255 ($C_{15}H_{15}N_2O_2$) could be explained as water and CO
486 loss from the carboxylic group, dehydration from one of the hydroxyl groups and
487 demethylation from the alkyl group. Similarly, fragment *m/z* 241 ($C_{14}H_{13}N_2O_2$)
488 corresponded to the demethylation of fragment *m/z* 255. Both fragments
489 suggested that the second hydroxyl group could not be lost, and to match with the
490 reductive defluorination proposed by Compound Discoverer, both OH groups
491 should be placed in adjacent carbons. Finally, oxidative deamination plus
492 reductive defluorination of CIPRO was proposed for BP33 (*m/z* 315.13394) . The
493 absence of *m/z* 70, together with the oxidative deamination and the loss of CO
494 (*m/z* 287), pinpointed the introduction of an aldehyde group in replacement of the
495 secondary amine of the piperazinyl ring. Fragment *m/z* 255 could be explained as
496 dehydration (-18) in the carboxyl group and demethylation (-14) in the *N*-ethyl
497 group of fragment *m/z* 287.

498 On the contrary to BP31-33, oxidative defluorination was pinpointed in BP34-35.
499 BP34 (*m/z* 345.14450) corresponded to the oxidative deamination, oxidative

defluorination plus methylation of CIPRO. Similar to BP32, the fragment *m/z* 317 indicated a CO loss from the precursor, suggesting the presence of an aldehyde formed during the oxidative deamination. Fragments *m/z* 283 and *m/z* 271 suggested the presence of the *N*-ethyl group formed after the cleavage of the piperazinyl ring. On the other hand, since methoxy group loss was not observed, the methoxy or hydroxyl group plus methyl groups should be located in the aromatic ring, being most probable the addition of the methoxy group to either the sp^2 carbon that contained the fluorine atom or to the adjacent one. Actually, since two regioisomers were detected, one could contain the methoxy group in the sp^2 carbon atom where the fluorine atom had been located and the other one could contain the methoxy group in the adjacent sp^2 carbon atom. Lastly, fragment *m/z* 327 was attributed to a water loss due to the presence of the carboxylic acid group of CIPRO, and this structure also explained the absence of fragment *m/z* 70 (C_4H_8N) and the presence of fragments *m/z* 74 (C_3H_8NO) and *m/z* 86 (C_4H_8NO). Finally, hydration, oxidative deamination to ketone plus oxidative defluorination of CIPRO was suggested to explain the metabolite BP35 (*m/z* 347.12377). The CO loss observed before dehydration (fragment *m/z* 273) suggested the presence of an aldehyde group formed from the cleavage of the piperazinyl ring and the oxidative deamination of the primary amine formed. The presence of the fragment *m/z* 301 attributed to a decarboxylation and the fragment *m/z* 287, corresponding to a subsequent dehydration, pinpointed that one hydroxyl group should be located in a position where dehydration could occur. Hence, we suggested a structure with a hydroxyl group in the aromatic ring (no water loss) and another one in the *N*-ethyl group formed during the cleavage of the piperazinyl ring. The -OH in the aromatic group should be related to defluorination but, with the

information available, we could not annotate its position, which could replace the fluorine atom or could be located in the adjacent sp^2 carbon. Lastly, the fragment *m/z* 241 ($C_{14}H_{13}N_2O_2$), which kept both nitrogen atoms of the precursor, could be explained by decarboxylation, CO loss from aldehyde, dehydration of the alcohol plus demethylation.

As above mentioned, defluorination was characteristic of all the BPs observed in bile, and BP31 was the most similar in structure to the 4 defluorinated BPs observed in seawater (BP2, BP5, BP9 and BP11). However, BP2, BP5 and BP9 were already present in the seawater in the absence of fish, therefore, BP31 was not necessarily their precursor. In the case of BP11, which was only present in the presence of fish, it could correspond to the oxidation of BP31.

3.3 Relative abundances of CIPRO BPs

In order to compare the abundances of BPs in the different scenarios studied, equivalent chromatographic signal response factors were assumed for all the BPs. Since response factors may differ among BPs, these results should be considered qualitative. Fig. S3 shows the relative abundances calculated as the ratio of the individual peak area with respect to the sum of all peak area in the different samples (seawater, seawater with fish and fish bile). All peak areas were corrected using internal standard ([$^2H_8$]-CIPRO).

CIPRO was significantly the most abundant compound in seawater in the absence and presence of fish, accounting for approximately the 95% of all the compounds detected in the aqueous phase. BP1 (*N*-formylation of CIPRO), BP4 (hydroxylation in the piperazinyl ring of CIPRO) and BP13 (*N*-formylation + esterification of CIPRO) were detected both in the absence and presence of fish in approximately 1% of the total compounds. In the presence of gilt-head bream, BP21 and BP24

were also detected at similar levels. The relative profile for CIPRO and BPs in seawater remained fairly consistent over the duration of the experiment regardless the presence or absence of fish. The BPs in the presence of fish correspond to the most complete scenario since we did not only consider the BPs formed in seawater due to photodegradation or degradation by microorganisms present in seawater but we also take into account those present in the seawater media due to either fish elimination or formation in the water media in the presence of fish excrements.

In the case of fish bile, BP32 was found at the highest abundance (33-58%), followed by CIPRO (18-26%) and BP33 (19-28%) and the relative profile varied with time. Overall, while a slight decrease of BP32 was observed with time, BP33 increased. An increase of BP34 up to 6% was also observed at day 3 of exposure, and BP31 (4%) and BP35 (3%) also increased in the last exposure day (day 8).

4. CONCLUSIONS

In order to assess risks associated with the exposure to PhACs in aquatic wildlife, a complete understanding of the uptake of the pharmaceutical together with its potentially bioactive BPs is required. Although this can vary from specie to specie and under different environmental conditions (seawater vs freshwater), in the present work it has been observed that CIPRO is only accumulated in gilt head bream bile and not in lipidic tissues.

On the other hand, even though CIPRO was significantly the most abundant compound in seawater, accounting for approximately the 95 % of all the compounds detected in the aqueous phase, 30 different BPs were detected in water and another different 5 BPs in fish bile. The fact of having just 14 BPs in

574 common in seawater in the absence and presence of fish clearly indicates that the
575 degradation of CIPRO is dependent on environmental conditions. It is worth
576 mentioning that in the BPs annotated in the presence of fish, oxidative
577 deamination and both glycine and glutamine conjugation gained importance. In the
578 case of bile, while glycine or glutamine conjugates were observed, defluorination
579 and oxidative deamination were relevant, with BP32 being even more abundant
580 than CIPRO. Lastly, with *in-silico* tests that concluded genotoxicity of CIPRO BPs
581 to bacteria and mammals, and having reported 30 BPs out of 35 for the first time in
582 the present work it is suggested that the identification of new BPs is a required
583 challenge in order to include the determination and effects of PhACs BPs in
584 environmental exposure assessment.

585 **5. ACKNOWLEDGEMENTS**

586 This work was financially supported by the Ministry of Economy and
587 Competitiveness through the project CTM2014-56628-C3-1-R. H. Ziarrusta is
588 grateful to the Spanish Ministry and L. Mijangos to the Basque Government for
589 their predoctoral fellowships. The research group is deeply acknowledged to
590 Plentzia Marine Station (PiE) and to its members for the facilities and their support.

591

592 **6. REFERENCES**

593 Alcaráz, M.R., Vera-Candioti, L., Culzoni, M.J., Goicoechea, H.C., 2014. Ultrafast
594 quantitation of six quinolones in water samples by second-order capillary
595 electrophoresis data modeling with multivariate curve resolution–alternating
596 least squares. Anal. Bioanal. Chem. 406, 2571–2580.
597 https://doi.org/10.1007/s00216-014-7657-3
598 Aryal, S., 2001. Antibiotic Resistance: A Concern to Veterinary and Human Medicine.
599 Nepal Agric. Res. J. 4, 66–70. https://doi.org/10.3126/narj.v4i0.4873
600 Ashfaq, M., Khan, K.N., Rasool, S., Mustafa, G., Saif-Ur-Rehman, M., Nazar, M.F., Sun, Q.,
601 Yu, C.-P., 2016. Occurrence and ecological risk assessment of fluoroquinolone

antibiotics in hospital waste of Lahore, Pakistan. Environ. Toxicol. Pharmacol. 42, 16–22. https://doi.org/10.1016/j.etap.2015.12.015

Babić, S., Periša, M., Škorić, I., 2013. Photolytic degradation of norfloxacin, enrofloxacin and ciprofloxacin in various aqueous media. Chemosphere 91, 1635–1642. https://doi.org/10.1016/j.chemosphere.2012.12.072

Burhenne, J., Ludwig, M., Spiteller, M., 1997. Photolytic degradation of fluoroquinolone carboxylic acids in aqueous solution. Environ. Sci. Pollut. Res. 4, 61–67. https://doi.org/10.1007/BF02986278

Carvalho, I.T., Santos, L., 2016. Antibiotics in the aquatic environments: A review of the European scenario. Environ. Int. 94, 736–757. https://doi.org/10.1016/j.envint.2016.06.025

Elston, R.A., Drum, A.S., Schweitzer, M.G., Rode, R.A., Bunnell, P.R., 1994. Comparative Uptake of Orally Administered Difloxacin in Atlantic Salmon in Freshwater and Seawater. J. Aquat. Anim. Health 6, 341–348. https://doi.org/10.1577/1548-8667(1994)006<0341:CUOOAD>2.3.CO;2

Erickson, R.J., McKim, J.M., Lien, G.J., Hoffman, A.D., Batterman, S.L., 2006. Uptake and elimination of ionizable organic chemicals at fish gills: I. Model formulation, parameterization, and behavior. Environ. Toxicol. Chem. 25, 1512–1521. https://doi.org/10.1897/05-358R.1

Gao, L., Shi, Y., Li, W., Liu, J., Cai, Y., 2012. Occurrence, distribution and bioaccumulation of antibiotics in the Haihe River in China. J. Environ. Monit. 14, 1247–1254. https://doi.org/10.1039/C2EM10916F

Gomes, M.P., Gonçalves, C.A., de Brito, J.C.M., Souza, A.M., da Silva Cruz, F.V., Bicalho, E.M., Figueredo, C.C., Garcia, Q.S., 2017. Ciprofloxacin induces oxidative stress in duckweed (Lemna minor L.): Implications for energy metabolism and antibiotic-uptake ability. J. Hazard. Mater. 328, 140–149. https://doi.org/10.1016/j.jhazmat.2017.01.005

Guo, H.-G., Gao, N.-Y., Chu, W.-H., Li, L., Zhang, Y.-J., Gu, J.-S., Gu, Y.-L., 2013. Photochemical degradation of ciprofloxacin in UV and UV/H2O2 process: kinetics, parameters, and products. Environ. Sci. Pollut. Res. 20, 3202–3213. https://doi.org/10.1007/s11356-012-1229-x

Haddad, T., Kümmerer, K., 2014. Characterization of photo-transformation products of the antibiotic drug Ciprofloxacin with liquid chromatography–tandem mass spectrometry in combination with accurate mass determination using an LTQ-Orbitrap. Chemosphere, PHARMACEUTICAL PRODUCTS IN THE ENVIRONMENT: FOR A MORE RELIABLE RISK ASSESSMENT 115, 40–46. https://doi.org/10.1016/j.chemosphere.2014.02.013

Hop, C.E.C.A., Prakash, C., 2005. Metabolite identification by LC-MS: applications in durg discovery and development, in Chowdhury, S.K. (ed.), Identification and Quantification of drugs, metabolites and metabolizing enzymes by LC-MS. Elsevier, Amsterdam, pp. 123-158.

Hu, L., Stemig, A.M., Wammer, K.H., Strathmann, T.J., 2011. Oxidation of Antibiotics during Water Treatment with Potassium Permanganate: Reaction Pathways and Deactivation. Environ. Sci. Technol. 45, 3635–3642. https://doi.org/10.1021/es104234m

Kovačević, B., Schorr, P., Qi, Y., Volmer, D.A., 2014. Decay mechanisms of protonated 4-quinolone antibiotics after electrospray ionization and ion activation. J. Am. Soc. Mass Spectrom. 25, 1974–1986. https://doi.org/10.1007/s13361-014-0972-2

651 Levy, S.B., 2002. Factors impacting on the problem of antibiotic resistance. J.
652 Antimicrob. Chemother. 49, 25–30. https://doi.org/10.1093/jac/49.1.25
653 Levy, S.B., 1997. Antibiotic resistance: an ecological imbalance. Ciba Found. Symp. 207,
654 1-9; discussion 9-14.
655 Maia, A.S., Ribeiro, A.R., Amorim, C.L., Barreiro, J.C., Cass, Q.B., Castro, P.M.L., Tiritan,
656 M.E., 2014. Degradation of fluoroquinolone antibiotics and identification of
657 metabolites/transformation products by liquid chromatography–tandem mass
658 spectrometry. J. Chromatogr. A 1333, 87–98.
659 https://doi.org/10.1016/j.chroma.2014.01.069
660 Morales-Gutiérrez, F.J., Hermo, M.P., Barbosa, J., Barrón, D., 2014. High-resolution
661 mass spectrometry applied to the identification of transformation products of
662 quinolones from stability studies and new metabolites of enrofloxacin in
663 chicken muscle tissues. J. Pharm. Biomed. Anal. 92, 165–176.
664 https://doi.org/10.1016/j.jpba.2014.01.014
665 Nallani, G.C., Edziyie, R.E., Paulos, P.M., Venables, B.J., Constantine, L.A., Huggett, D.B.,
666 2016. Bioconcentration of two basic pharmaceuticals, verapamil and clozapine,
667 in fish. Environ. Toxicol. Chem. 35, 593–603.
668 https://doi.org/10.1002/etc.3244
669 Paul, T., Dodd, M.C., Strathmann, T.J., 2010. Photolytic and photocatalytic
670 decomposition of aqueous ciprofloxacin: Transformation products and
671 residual antibacterial activity. Water Res. 44, 3121–3132.
672 https://doi.org/10.1016/j.watres.2010.03.002
673 Pereira, V.J., Linden, K.G., Weinberg, H.S., 2007. Evaluation of UV irradiation for
674 photolytic and oxidative degradation of pharmaceutical compounds in water.
675 Water Res. 41, 4413–4423. https://doi.org/10.1016/j.watres.2007.05.056
676 Prieto, A., Möder, M., Rodil, R., Adrian, L., Marco-Urrea, E., 2011. Degradation of the
677 antibiotics norfloxacin and ciprofloxacin by a white-rot fungus and
678 identification of degradation products. Bioresour. Technol. 102, 10987–10995.
679 https://doi.org/10.1016/j.biortech.2011.08.055
680 Ramanathan, R., Chowdhury, S.K., Alton, K.B., 2005. Oxidative metabolites of drugs
681 and xenobiotics: lc-ms methods to identify and characterize in biological
682 matrices, in Chowdhury, S.K. (ed.), Identification and Quantification of drugs,
683 metabolites and metabolizing enzymes by LC-MS. Elsevier, Amsterdam, pp.
684 225–276.
685 Salma, A., Thoröe-Boveleth, S., Schmidt, T.C., Tuerk, J., 2016. Dependence of
686 transformation product formation on pH during photolytic and photocatalytic
687 degradation of ciprofloxacin. J. Hazard. Mater. 313, 49–59.
688 https://doi.org/10.1016/j.jhazmat.2016.03.010
689 Schymanski, E.L., Jeon, J., Gulde, R., Fenner, K., Ruff, M., Singer, H.P., Hollender, J., 2014.
690 Identifying Small Molecules via High Resolution Mass Spectrometry:
691 Communicating Confidence. Environ. Sci. Technol. 48, 2097–2098.
692 https://doi.org/10.1021/es5002105
693 Toolaram, A.P., Haddad, T., Leder, C., Kümmerer, K., 2016. Initial hazard screening for
694 genotoxicity of photo-transformation products of ciprofloxacin by applying a
695 combination of experimental and in-silico testing. Environ. Pollut. 211, 148–
696 156. https://doi.org/10.1016/j.envpol.2015.12.040
697 Turiel, E., Bordin, G., Rodríguez, A.R., 2005. Determination of quinolones and
698 fluoroquinolones in hospital sewage water by off-line and on-line solid-phase

699 extraction procedures coupled to HPLC-UV. J. Sep. Sci. 28, 257–267.
700 https://doi.org/10.1002/jssc.200400018
701 Van Doorslaer, X., Dewulf, J., Van Langenhove, H., Demeestere, K., 2014.
702 Fluoroquinolone antibiotics: An emerging class of environmental
703 micropollutants. Sci. Total Environ. 500–501, 250–269.
704 https://doi.org/10.1016/j.scitotenv.2014.08.075
705 Vasconcelos, T.G., Henriques, D.M., König, A., Martins, A.F., Kümmerer, K., 2009.
706 Photo-degradation of the antimicrobial ciprofloxacin at high pH: Identification
707 and biodegradability assessment of the primary by-products. Chemosphere 76,
708 487–493. https://doi.org/10.1016/j.chemosphere.2009.03.022
709 Villegas-Guzman, P., Oppenheimer-Barrot, S., Silva-Agredo, J., Torres-Palma, R.A.,
710 2017. Comparative Evaluation of Photo-Chemical AOPs for Ciprofoxacin
711 Degradation: Elimination in Natural Waters and Analysis of pH Effect, Primary
712 Degradation By-Products, and the Relationship with the Antibiotic Activity.
713 Water. Air. Soil Pollut. 228, 209. https://doi.org/10.1007/s11270-017-3388-3
714 Wetzstein, H.-G., Stadler, M., Tichy, H.-V., Dalhoff, A., Karl, W., 1999. Degradation of
715 Ciprofloxacin by Basidiomycetes and Identification of Metabolites Generated
716 by the Brown Rot Fungus Gloeophyllum striatum. Appl. Environ. Microbiol. 65,
717 1556–1563.
718 Zhang, X., Li, R., Jia, M., Wang, S., Huang, Y., Chen, C., 2015. Degradation of
719 ciprofloxacin in aqueous bismuth oxybromide (BiOBr) suspensions under
720 visible light irradiation: A direct hole oxidation pathway. Chem. Eng. J. 274,
721 290–297. https://doi.org/10.1016/j.cej.2015.03.077
722 Zhao, J.-L., Liu, Y.-S., Liu, W.-R., Jiang, Y.-X., Su, H.-C., Zhang, Q.-Q., Chen, X.-W., Yang, Y.-
723 Y., Chen, J., Liu, S.-S., Pan, C.-G., Huang, G.-Y., Ying, G.-G., 2015. Tissue-specific
724 bioaccumulation of human and veterinary antibiotics in bile, plasma, liver and
725 muscle tissues of wild fish from a highly urbanized region. Environ. Pollut. 198,
726 15–24. https://doi.org/10.1016/j.envpol.2014.12.026
727 Ziarrusta, H., Val, N., Dominguez, H., Mijangos, L., Prieto, A., Usobiaga, A., Etxebarria, N.,
728 Zuloaga, O., Olivares, M., 2017. Determination of fluoroquinolones in fish
729 tissues, biological fluids, and environmental waters by liquid chromatography
730 tandem mass spectrometry. Anal. Bioanal. Chem. 1–12.
731 https://doi.org/10.1007/s00216-017-0575-4
732

Universidad del País Vasco Euskal Herriko Unibertsitatea
ZIENTZIA ETA TEKNOLOGIA FAKULTATEA
FACULTAD DE CIENCIA Y TECNOLOGÍA

- First uptake/biotransformation study with ciprofloxacin-exposed gilt-head bream
- Ciprofloxacin and its by-products (BPs) were only observed in gilt-head bream bile
- Up to 35 BPs (30 novel structures) were annotated in seawater and bile using HRMS
- Different ciprofloxacin degradation pathway was found in presence and absence of fish
- Besides pharmaceuticals, BPs should also be considered for risk assessment studies

Department of Analytical Chemistry
Faculty of Science and Technology
University of the Basque Country
Barrio Sarriena s/n, 48940 Leioa, Spain

Tel.: +34 94 601 55 51
Fax: +34 94 601 35 00
e-mail: haizea.ziarrusta@ehu.eus